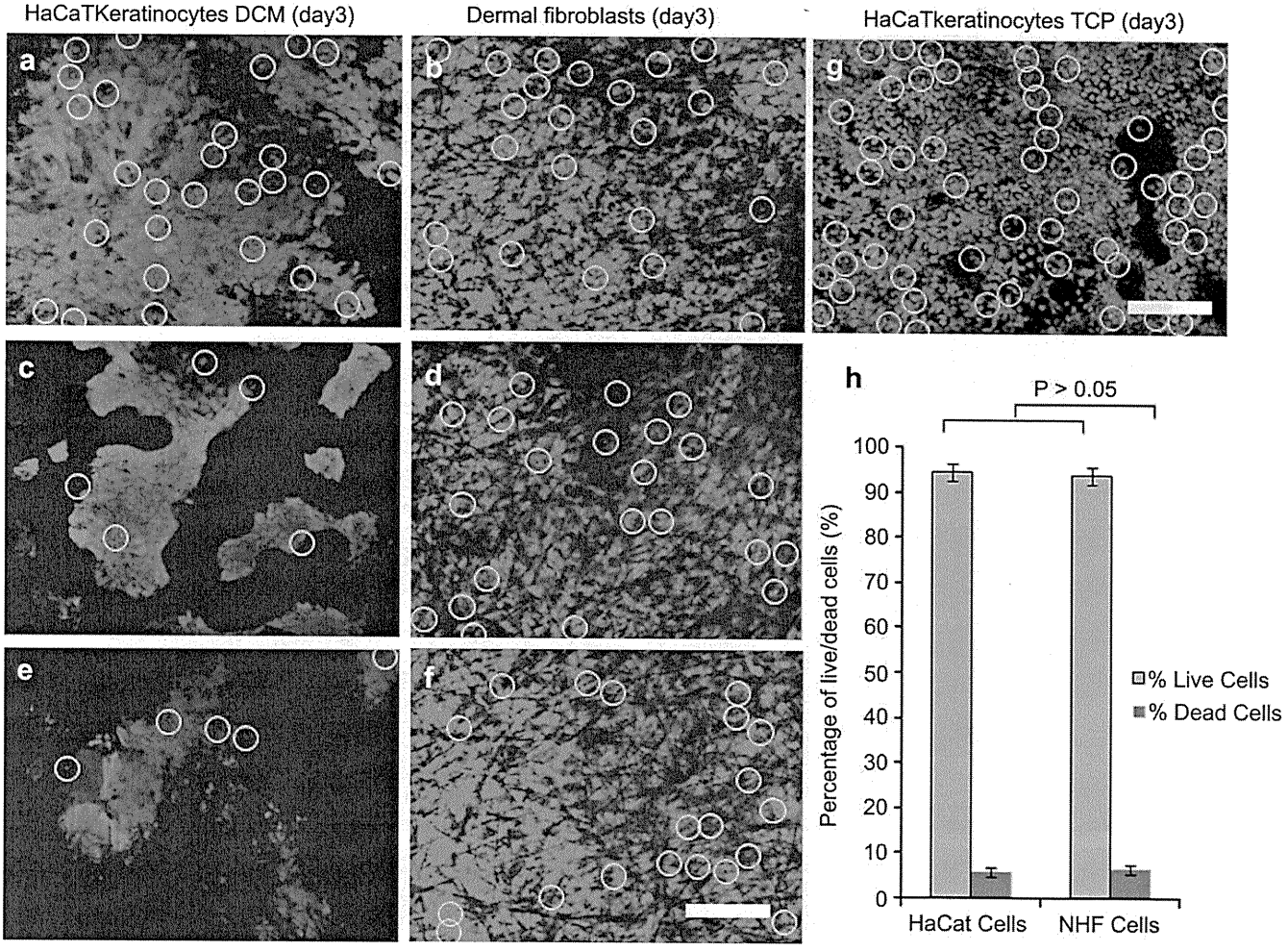


**Fig. 1.** Both HaCaT keratinocytes (a, c, e) and normal human dermal fibroblasts (b, d, f) exhibited variable cell densities on the same denatured collagen microfiber (DCM) and could adhere and survive under standard cell culture conditions. HaCaT keratinocytes (green cell in a, c, e) exhibited variable-sized islands of cultured cells with very little evidence of cell migration over or penetration into the core the of DCM biomaterial fibers. Small numbers of individual dead keratinocyte or fibroblasts were apparent (highlighted by white circles over dead cells stained red in a–g). Conversely, fibroblasts demonstrated evidence of cell spreading and migration over and penetration within the entire DCM biomaterial (as highlighted by live cell confocal green fluorescent signal being interrupted by non-fluorescent DCM fibers in b, d, f). This is in contrast to uninterrupted staining of cells (HaCaT or fibroblasts, g) maintained on tissue culture plastic (TCP). Scale bar 200 μm. Image analysis of these images produced estimates of over 94% cell viability (and around 5% non viable cells) for both cell types maintained on DCM biomaterial (HaCaTs 94.3%, fibroblasts 93.6% viable). (For interpretation of the references to colour in this figure legend, the reader is referred to the web version of this article).

Samples were cut, stained with uranyl acetate and lead citrate and viewed under a JEOL 1010 transmission electron microscope at 75–80 kV with digital image capture.

### 2.6. Assessment of DCM biomaterial wound biocompatibility in immunocompetent mice

These two procedures, experiments 1 and 2 were performed based on a previous protocol [33]. All animal procedures were conducted according to guidelines provided by the appropriate University Biomedical Institutional Animal Ethics Committee under an approved protocol governing the use of experimental animals. For experiment 1, DCM biomaterial was grafted onto two groups ($n = 5$ each) of 6 week old BALB/cA Jcl immunocompetent mice to assess the effect of the DCM scaffold on excisional wounding without the presence of any human cells (DCM treated or control untreated). The mice were anesthetized with a intra peritoneal (i.p.) injection of 50 mg/kg Ketamine/10 mg/kg Xylasil with additional top-up isofluorane anesthetic as required (0.5–2% isofluorane flow rate of $O_2$ at 0.5–0.75L/min). The dorsal fur was clipped, ethanol cleaned and a 4 mm diameter full-thickness excisional punch biopsy (Provet, Pty Ltd, Australia) wound made through the back skin. A 4 mm punch biopsy disc of DCM biomaterial was placed and secured within the boundary of original excisional wound or left untreated as a control. All the wounds were then immediately dressed with occlusive film (GLAD Wrap ©, Padstow, NSW Australia) to maintain the wound in a moist environment and held in place for 1 week by Fixomull bandage (Smith and Nephew Healthcare, Hull, UK). After 7 days the dressings were removed and the dimensions of each wound were then digitally photographed and recorded on a daily basis and wound closure rates assessed using image analysis software (Image Pro Plus V9, Media Cybernetics, Bethesda, MD, USA). Wound closure was defined as the point when the epidermal skin surface appeared completely re-epithelialized (closed) with no evidence of underlying tissue such as bodily secretions, exudate or crusted blood. Wound size and closure rates were calculated by converted pixel area to wound area in $mm^2$ until complete re-epithelialization had taken place (performed in a standardized fashion by one individual). All wounds were repaired within 18 days. After 21 days the mice were sacrificed by $CO_2$ asphyxiation and the remaining dorsal skin shaved. The centre of each wound was then labeled with indelible (permanent) marker and the biopsy excised with a 20–50 mm border of normal skin (for orientation purposes) processed for histological examination.

### 2.7. Assessment of DCM cell composites on wound healing in immunosuppressed mice

In mouse experiment 2, we assessed the effects of different combinations of cell-DCM biomaterial composites in our excisionally wounded SCID (C.B-17 Icr-Scid Jcl strain on a BALB/c background) model mice using five groups of 6 week old immunodeficient mice ($n = 5$ per group, 35 in total) were included in this experiment. The mice were prepared and treated as previously described but each group was treated with a different biomaterial composite wound insert. The groups comprised 1) wounded untreated mice, 2) wounded/DCM/nylon nylon Mersilene™ nylon mesh support(mesh) treated mice, 3) wounded/mesh support alone treated

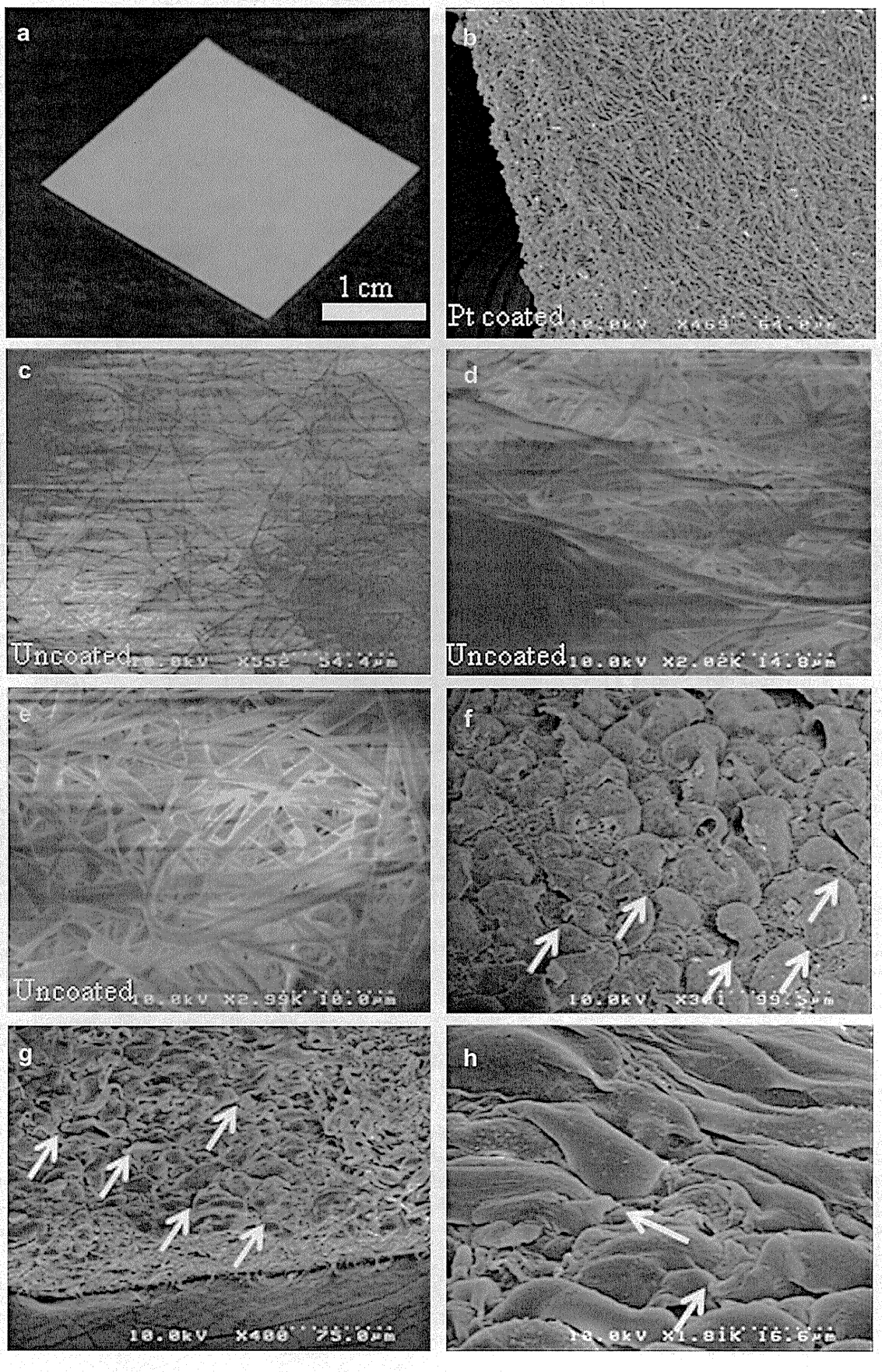

mice and 4) wounded/DCM/mesh/HaCaT/fibroblast and 5) wounded/DCM/mesh/NHEK/fibroblast human skin equivalent treated SCID mice (see previous methods section for details of cell-DCM biomaterial culture). Wounds were dressed for 1 week only and wound closure assessment made from day 7 until complete re-epithelialization. Macroscopic wound photographic results from individual animals and averaged group results of closure rates and total time to wound closure from each treatment group of animals were assessed using image analysis software (Image Pro Plus V9, Media Cybernetics, Bethesda, MD, USA) and displayed graphically. All mice were sacrificed on day 21 and wound biopsies taken for histological assessment as described below.

### 2.8. Immunohistological wound assessment

Fur-clipped, indelibly marked wounded mouse skin and surrounding, perilesional unwounded skin were removed and either embedded in OCT compound (SAKURA, Torrance, CA) to be snap frozen in liquid nitrogen cooled isopentane or fixed in 4% formaldehyde in phosphate buffered saline, and processed for paraffin embedding for routine H&E and modified Masson's Trichrome stains for histological analysis (to assess wound healing responses, fibrosis and identify areas of neodermis containing newly synthesized collagen). Wounds were assessed by multiple serial sectioning and selection of tissue from the closest point to the center of the wound.

To assess the persistence and migration of human cells delivered into mouse wound tissue from the biomaterial graft in the SCID mouse model we performed indirect immunofluorescence using frozen, unfixed cryostat sections of mouse wounded skin treated with cell-biomaterial composites and normal human skin sections as controls. Briefly, cryostat tissue sections were fixed in acetone and incubated with primary antibody/antisera. Sections were incubated with secondary antibodies conjugated to fluorescein isothiocyanate (FITC; rabbit anti-mouse IgG or goat anti rabbit IgG; 1: 200; Dako, Tokyo, Japan). Sections were then labeled with a 4′,6-diamidino-2-phenylindole (DAPI) nuclear counter stain contained in Vectashield mounting medium (Vectorlabs, Burlingame, CA, USA). The sections were examined with an Olympus Fluoview FV300 confocal microscope (Olympus, Tokyo, Japan) in duplicate. Controls included human skin cryostat sections with the primary antibody substituted by PBS, myeloma supernatant or an irrelevant immunoglobulin isotype, as a negative control. All experiments were performed in duplicate.

### 2.9. Statistical analysis

For quantitative measurements either the Student's *t*-test for two sample comparison or for multiple comparison ANOVA was performed (Minitab Incorporated, University of Pennsylvania, Philadelphia, PA, USA) at a $P$ value $< 0.05$ or $< 0.01$ to demonstrate significance.

## 3. Results

### 3.1. Livedead® cell assay

The results show that DCM scaffold is able to maintain adhesion and cell survival of both keratinocyte HaCaT cells (Fig. 1a, c, e) and fibroblasts on DCM (Fig. 1b, d, f) in a similarly effective fashion as cells cultured on conventional tissue culture plastic (TCP) (g). There were however, two main differences between keratinocyte and fibroblast migration on DCM compared to TCP. Firstly, keratinocyte cells formed discrete islands over a limited area on the DCM surface suggesting that lateral migration over the surface of DCM is severely limited or completely inhibited compared to fibroblasts (Fig. 1a, c, e versus b, d, and f). Secondly, migration of the primary human fibroblasts into the DCM matrix was much more evident as demonstrated by the pattern of dark 2-5 μm-thick fibers crossing the images obscuring the live (green fluorescent) cells in the center of the DCM biomaterial (Fig. 1b, d, f) compared to the unobscured keratinocytes (Fig. 1a, c, e). For each cell type the percentage of viable cells (in green) was very high and ranged between (94–96% viability) with HaCaT keratinocyte cells demonstrating a similar mean viability to fibroblasts on DCM (Fig. 1h $p > 0.05$) or compared to HaCaTs maintained on polystyrene TCP (96.2% live see Fig. 1g). Dead cells in the Livedead® assay were shown as small dots stained in red (highlighted by white circles a–g). Due to limitations in HaCaT keratinocyte monolayer cell migration over DCM (shown by their preponderance to remain in small islands) and to induce stratification primary human keratinocytes were included in subsequent experiments.

### 3.2. Scanning electron microscopy

Gross macroscopic analysis of the DCM biomaterial demonstrated a thin, moderately stiff white, paper-like fibrous biomaterial (Fig. 2a) that became softer and more pliable upon immersion in aqueous solutions. Low power scanning electron microscopy (SEM) of platinum coated samples revealed a complex multilayered fibrous structure comprising a compact network of randomly oriented (non-woven) fibers of various thicknesses ranging in diameter from 2 to 5 μm (mean diameter of 4.3 μm, $n = 50$ fibers) and with variable inter-fiber porosity ranging between 3 and 10 μm (mean 6.7 μm, $n = 50$ fibers). This considerable range in DCM fiber diameter (up to 2.5 fold) coupled with variable porosity are crucial design characteristics of this biomaterial [9,24]. Overall the entire thickness of the DCM biomaterial ranged between 50 and 70 μm (Fig. 2b) and visualization into the upper 10–20 μm layers of fibers of this fibrous sheet was possible in uncoated samples (i.e. without Pt coating, Fig. 2c–e). DCM cell composites demonstrated normal primary human epidermal keratinocyte (NHEK)(Fig. 2f), HaCaT keratinocyte cell line (Fig. 2g) and fibroblast cell (Fig. 2h) attachment and spreading on the fibrous biomaterial surface. Cell membrane processes involved the formation of lamellapodia and putative sites of focal contact formation were observed (see white arrows in Fig. 2f–h).

### 3.3. Transmission electron microscopy

Semithin sections of normal human skin demonstrated multilayered, keratinizing epidermal layers and bundles of well organized collagen fibers in the dermis (labeled D in Fig. 3a). Plastic embedded, sectioned biomaterial (Fig. 3b) and skin cell-biomaterial composites (Fig. 3c–g) demonstrated that DCM is a good dermal substitute allowing keratinocyte and fibroblast cell adhesion/survival and fibroblast migration over and penetration into the DCM biomaterial. DCM comprised a more amorphous aggregation of randomly distributed and oriented electrospun fibers (Fig. 3b). Despite this, normal primary human epidermal keratinocytes (NHEK) (Fig. 3c), HaCaT keratinocyte cells (Fig. 3d) and normal fibroblasts (Fig. 3e) all adhered directly on to the DCM scaffold. Furthermore, fibroblasts migrated into the DCM when cultured either alone or co-cultured with HaCaT keratinocyte cells (Fig. 3e and f). Co-cultures of HaCaT and fibroblasts on DCM (Fig. 3f), however, failed to form a multilayered, well stratified and keratinized epidermal layer, despite the

**Fig. 2.** Macroscopic and electron microscopic views of denatured collagen microfiber (DCM) biomaterial without seeded cells (a–e) and with seeded skin cells (keratinocytes f, g and fibroblasts h). Macroscopic view of DCM biomaterial reveals a variably stiff but thin white fibrous material resembling a good quality slightly thickened paper sheet that becomes soft and flexible when hydrated (a). Scanning electron microscopy (SEM) of Pt coated DCM shows a dense network of randomly interwoven fibers with a well defined, almost solid surface that upon closer SEM inspection of uncoated samples (hence the DCM biomaterial exhibited some static charging effects) revealed a network of large pores (between 3 and 10 μm mean 6.7 μm) and channels between loose, randomly oriented electrospun DCM fibers 2–5 μm in thickness (c–e) with a mean fiber diameter of 4.3 μm. HaCaT and primary keratinocytes (f and g) and fibroblasts (h) were seeded on DCM and maintained in culture for between 3 and 8 days. Keratinocytes formed small rounded, dome shaped cells with cytoplasmic focal contact projections resembling lamellapodia extending toward the DCM surface. Fibroblasts however, formed longer, thinner elongated cells with fewer, typically 3–4 focal contact like projections at the ends of lamellapodia. Several small sections of fibroblasts were observed protruding from within the DCM channels and pores (data not shown).

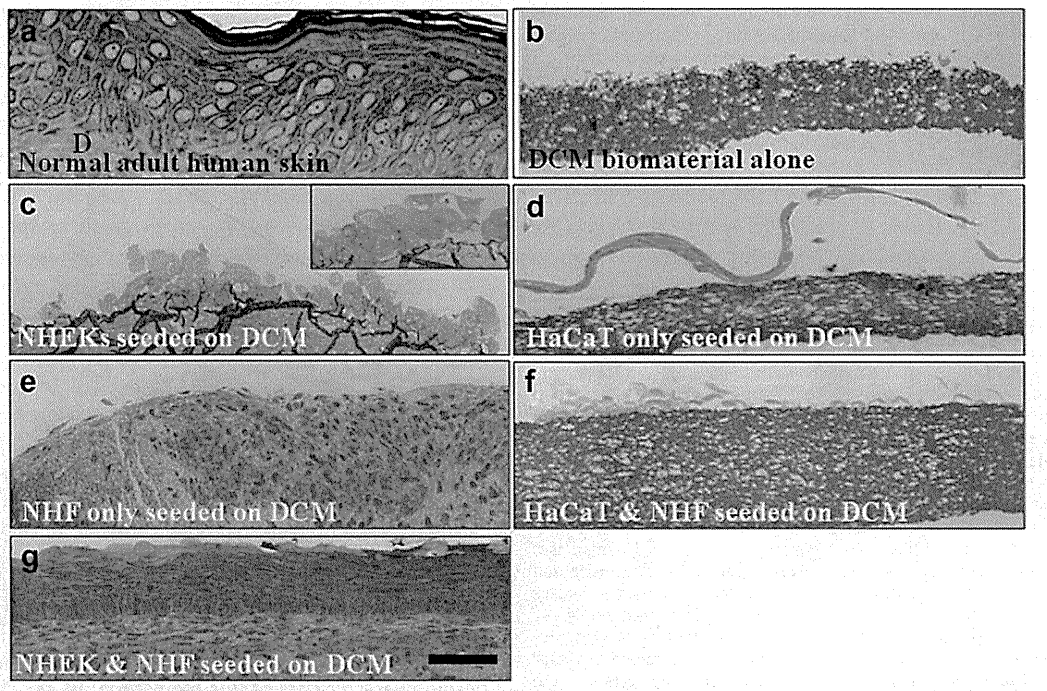


**Fig. 3.** Semithin plastic embedded sections show normal human skin (a) with stratified, keratinized epidermal layers over lying bundles of dermal collagen (labeled as D in a), whereas the structure of DCM scaffold (b) is more amorphous and significantly thinner than human dermal tissue with a thickness of between 50 and 70 μm. Cell-biomaterial composites show that primary keratinocytes (c) HaCaT cells (d)/and fibroblasts (e) adhere to DCM scaffolds (b) and can be maintained in culture. Seeded primary (c) and HaCaT (d) keratinocyte monocultures adhere to DCM with the formation of thin multilayered epidermal keratinocytes in culture. Fibroblasts, however, proliferate (more than any of the keratinocyte cell types) over the surface of the DCM and in addition penetrate the porous DCM fibers in culture (e). co-culture of HaCaT and fibroblast cells led to a loss of epidermal architecture and increases in HaCaT/fibroblast-DCM penetration (f). Conversely, co-culture of primary NHEKs and fibroblasts on DCM over 26 days at the air liquid interface (g) demonstrated remarkable levels of epidermal stratification and differentiation in addition to fibroblast invasion into the DCM substrate. Scale bar 150 μm. (For interpretation of the references to colour in this figure legend, the reader is referred to the web version of this article).

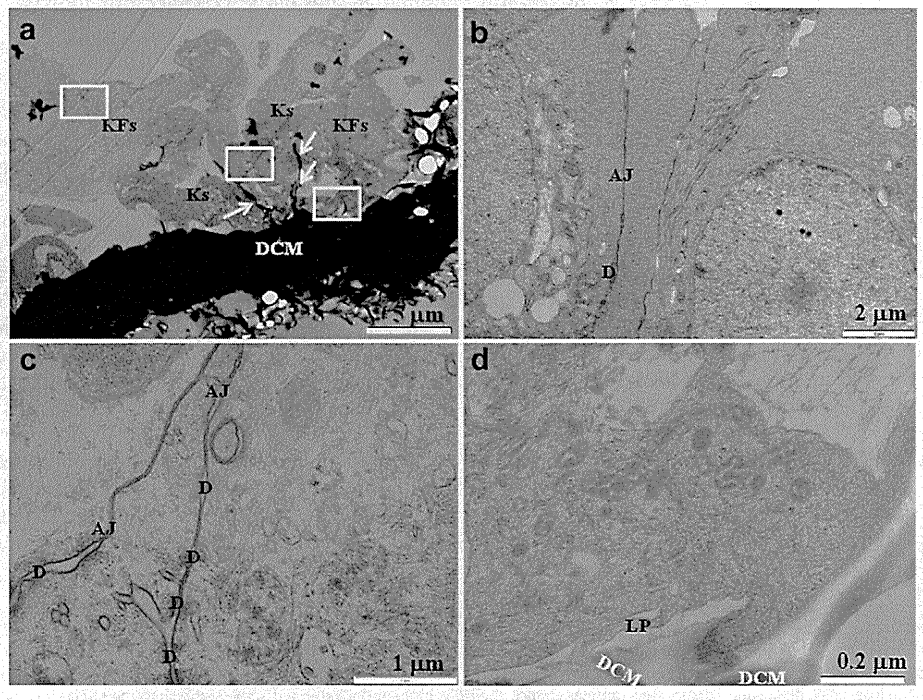


**Fig. 4.** Ultrastructural examination of primary human keratinocytes seeded on DCM showed a multilayered keratinocyte cell sheet attached to an electron dense DCM scaffold. Thin electron dense DCM fiber projections (white arrows in a) were noted between basal keratinocyte cells (Ks) close to the DCM scaffold (DCM). (b) In areas of close keratinocyte cell apposition highlighted by the middle white box in (a) there were cell–cell desmosomal junctions (labeled D) and adherens junctions (AJ). In areas these structures were quite numerous (left hand box in a, shown in c). However, in areas of keratinocyte-DCM apposition (right hand white box in a, shown in d) there were no signs of any hemidesmosomes linking the DCM substratum (d) only lamellapodia (LP) with putative focal contact like junctions.

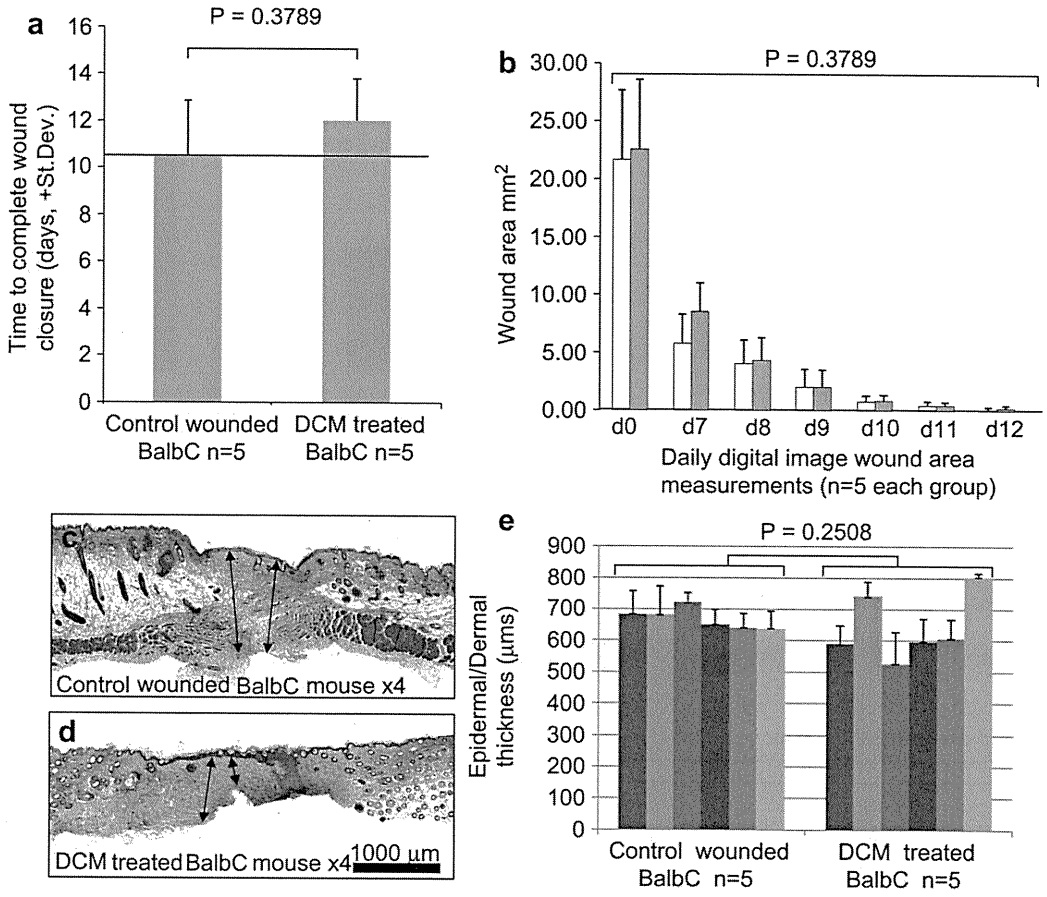


**Fig. 5.** Excisionally wounded immunocompetent BalbC model mice showed no difference in mean time to complete wound closure (a) or in the mean rate of wound closure (b) with or without DCM scaffold wound treatment ($n = 5$ each group). Furthermore, the effect of DCM scaffold incorporation into the healing excisional wound failed to induce significant foreign body wound immunoreactivity or scarring response as demonstrated by increases in the mean thickness of either wounded epidermal or dermal tissue (new collagen deposition stains blue see arrows in c and d) in modified Masson's Trichrome stained paraffin embedded mouse skin sections. Individual wound thickness measurements for each of the 5 BalbC mice per group demonstrated no alterations in wound thickness between treatment groups ($p > 0.251$). (For interpretation of the references to colour in this figure legend, the reader is referred to the web version of this article).

composite being raised to air–liquid interface on mesh supports and the DCM scaffold acting as a dermal substitute for fibroblast invasion. Conversely, co-culture of fibroblast and NHEK cells produced, 4–5 cell multilayered, polarized, well stratified and partially keratinized epidermal-like continuous structure (Fig. 3g). Ultrastructurally, the NHEK keratinocytes on the DCM exhibit good close cell–cell association with the presence of perinuclear keratin filaments (KFs, Fig. 4a) that upon higher magnification reveal closely apposing adjacent keratinocyte plasma membranes (Fig. 4b) with both desmosomal (D) and adherens junction (AJ) like structures on the membrane (Fig. 4c). On the basal border of the basal layer keratinocyte over lying the biomaterial (labeled DCM in Fig. 4d)there is a marked absence of hemidesmosomal cell-matrix junctions but instead there is are small membrane like lamellapodia-like processes consistent with the presence of focal contract cell-matrix junctions (LP in Fig. 4d).

### 3.4. Wounded model mice

Our data show from experiment 1 assessing the biocompatibility of DCM in BalbC mice demonstrated the incorporation of DCM scaffold without cells into wounded mouse tissue on immunocompetent mice has little or no adverse effect on the processes of normal wound healing and subsequent wound closure times in all 5 mice tested in each treatment group (Fig. 5a, $p > 0.05$) and rates of wound closure (Fig. 5b, $p > 0.05$). There was little difference in wound appearance between each of the different treatment groups with the main difference being slight changes in the rate of wound healing.

Both hematoxylin and eosin (H&E, data not shown) and modified Masson's Trichrome stained paraffin sections of mouse skin (Fig. 5c and d) showed similar re-epithelialization rates (Fig. 5a and b) and levels of skin thickening, 21 days after excisional wounding in both untreated and DCM treated mouse groups (Fig. 5e). Furthermore, there was no statistical difference in combined mean epidermal and dermal wound thickness (suggestive of scarring likelihood) over the excisional wounds themselves at 21 days post wounding (Fig. 5e).

Similarly, in experiment 2 assessing the efficacy of combinations of cell-DCM-scaffold composites in SCID mice there was no difference in mean would closure times (Fig. 6b, $p > 0.05$) or wound closure rates (Fig. 8) between the 5 treatment groups seeded with or without combinations of human fibroblast and keratinocyte-DCM grafts in our SCID mouse animal model. Normal human skin was used as the positive control from anti-human HLA staining (see asterisks in Fig. 7a) for human cells in mouse wounds. Confocal microscopy using anti-human HLA antibody staining of wounded mouse skin after treatment with 2 of the 5 graft combinations including human cells on DCM scaffold demonstrated that these cells were engrafted into the wounded mouse tissue, survive and were maintained there for up to 21 days post injury (see asterisks in Fig. 7e and f verses Fig. 7b–d).

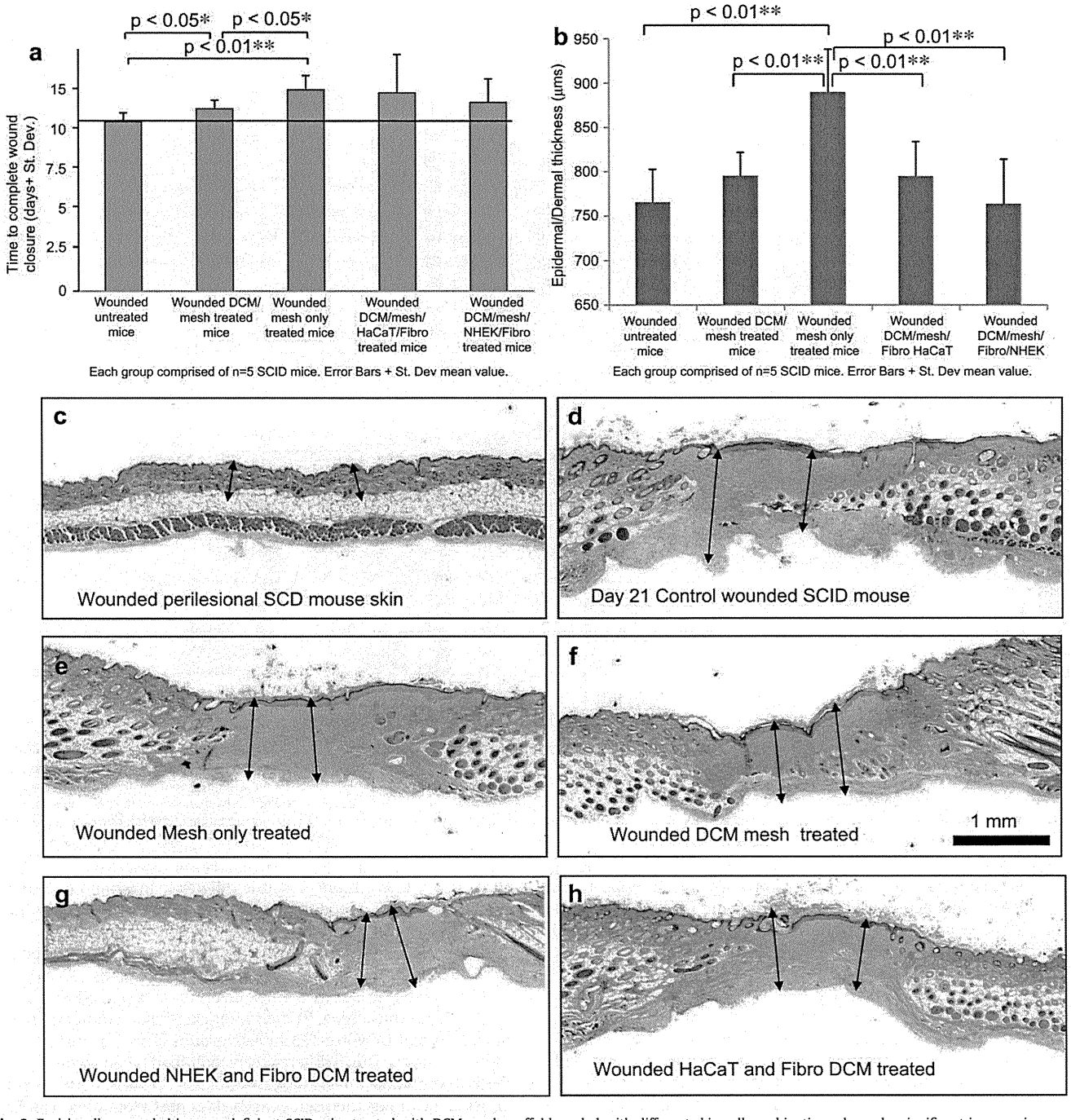


**Fig. 6.** Excisionally wounded immunodeficient SCID mice treated with DCM-mesh scaffold seeded with different skin cell combinations showed a significant increase in wound closure time compared to wound only, DCM and mesh treated and mesh treated wounds (a, $n = 5$ mice for each treatment group). There was no difference in the mean time to complete wound closure between the wound only, and the two DCM/mesh/skin cell-treated groups. Assessment of foreign body wound immunoreactivity/acute scarring response by using the mean combined epidermal/dermal tissue thickness (µm) 21 days after wounding demonstrated that the use of plastic mesh to support the graft at the air liquid interface during culture (and its subsequent incorporation into the DCM graft) increased acute wound thickness compared to all other treatments (b). This effect however, could be partially alleviated using DCM/mesh composite seeded with human skin cells (b). Histological analysis of paraffin embedded modified Masson's Trichrome stained wounded mouse skin demonstrated that compared to normal unwounded dermal thickness (c, mean depth 190 µm), the dermal wound thickness increased more than four fold in the untreated group (b and d), and by significantly more ($p < 0.01$) in the mesh treated group (graph in b and figures c and d versus e). All other wound treatments showed minimal affects on acute phase dermal thickening in the presence of DCM (with or without cells) with concomitant significant reductions in mesh-associated dermal scarring. Scale bar 1 mm or 1000 µm (c–h). (For interpretation of the references to colour in this figure legend, the reader is referred to the web version of this article).

## 4. Discussion

The material properties of electrospun denatured collagen microfiber (DCM) make this a promising candidate scaffold for skin-derived cell grafting. It comprises extracted bovine collagen and when combined with cells in a composite, avoids adverse foreign body immune responses after grafting more than many typical artificial polymers [9,21,34]. Bovine collagen was easy and cheap to prepare and quick to manufacture on an appropriate scale using a previously described process of acid extraction and

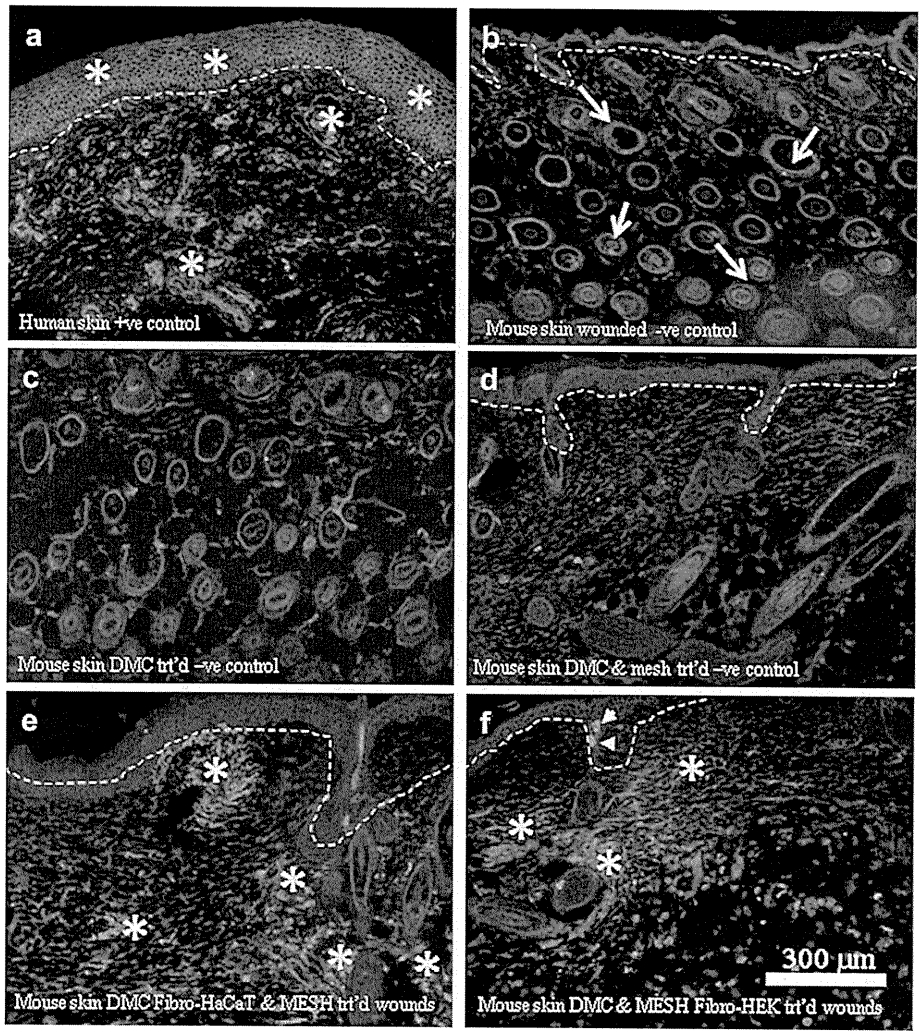


**Fig. 7.** Excisionally wounded SCID mice demonstrated human keratinocyte and fibroblast cell engraftment and survival in wounded mouse skin after 21 days using anti-human HLA specific antibodies after human cultured cell-DCM composite wound graft treatments. Control human skin stained with anti-human HLA antibody (a) showed bright fluorescence throughout the epidermis (asterisks above the dashed line) and bright patches within dermal tissue (asterisks). Conversely, untreated wounds (b), DCM (c), DCM/mesh only treated (d) mouse skin showed no focal areas of fluorescent staining for human keratinocyte or fibroblasts. However, non-specific reactivity with the antibody stained the hair follicle and shaft in many of these mouse tissues (see arrows in b). Finally, treatment of wounds with human HaCaT-fibroblasts (e) or primary keratinocyte-fibroblast DCM grafts (f) demonstrated significant staining of dermal cell foci (asterisks in e and f) and some epidermal staining (arrowheads in f) highlighting human cell survival and engraftment into the wound. Scale bar 0.3 mm or 300 µm (a–f). (For interpretation of the references to colour in this figure legend, the reader is referred to the web version of this article).

alcohol/UV sterilization to minimize potential biosafety issues but preserve, as much as possible, the natural collagen protein conformation [21]. Electrospinning was used to produce biomimetic-scaled scaffold fibers similar to dermal collagen fibers specific for this application. Such scaffold fibers mimic the close structural profile of the natural dermal extracellular matrix (ECM) to which the fibroblast and keratinocyte integrin receptors bind [21,35,37]. In addition, this scaffold was predicted and shown to be able to undergo complete hydrolysis during the dermal reorganizational and maturation stages of wound healing to become safely degraded in its target tissue. This avoids the need for the composite to be removed after grafting allowing the wound to remain intact avoiding further damage and subsequent inflammatory processes.

Electrospun collagen provides a porous, dermal-like template for skin cell attachment that allows both keratinocytes and fibroblasts to survive and proliferate and for fibroblasts to penetrate through and migrate over this scaffold *in vitro*. The uncoated DCM scaffold EM data suggest DCM pores average 6–7 µm (ranging from 3 to 10 µm) that are significantly larger than the lower cut-off limit described for fibroblast penetration and migration (anything smaller than between 4.5 and 5 µm limits fibroblast penetration) [9,24]. Conversely, these large DCM pores do not appear to encourage single cell keratinocyte or cell sheet migration/penetration as seen in fibroblasts. However, it appears that two factors may be able to overcome this reduced keratinocyte migration on DCM; firstly a high initial keratinocyte seeding density and secondly pre-seeding the DCM with live human fibroblasts until confluent. This migration finding was unexpected as keratinocytes failed to assemble hemidesmosomes that encourage stable anchorage to the underlying matrix-scaffold (likely due to the lack of laminin 332) but assembled multiple focal contact associated lamellapodia important in migration. We hypothesize that either cell type releases matrix or utilizes exogenous soluble factors that encourage keratinocyte focal contact adhesion when maintained on DCM scaffolds.

DCM scaffold appears efficient at maintaining cell adhesion and survival (compared to TCP substrates), however these precise adhesion rates are difficult to determine in our experiments since cell proliferation and survival might have affected the results

during the course of the Livedead® experiments. Previous studies have demonstrated that electrospun collagen fibers show reduced keratinocyte adhesion compared to unprocessed collagen or spun collagen fibers coated with ECM substrates [22,35]. In our experiments however, no deficit was noted in keratinocyte adhesion to fibroblast seeded DCM scaffold maintained in culture. These findings may reflect fibroblast cell deposition of new cell-matrix components (collagen I or fibronectin or vitronectin) onto the DCM scaffold before keratinocyte seeding as has been described for other scaffolds [9].

The porous nature of this scaffold and its ability to hold fluid between the fibers by capillary action means that graft survival can at least be temporarily supported by nutrients in wound tissue fluid, in the absence of a viable dermal blood supply. The ability of tissue fluid to support the graft would be made easier with a reduced cellular load in or on the scaffold, perhaps if grafted before complete confluence and/or epidermal maturation has taken place.

Conversely, the large 3-dimensional and variable pore sizes allow the reciprocal movement of both live fibroblast cells and cell-secreted cytokine growth factors into the wound bed to influence the important dermal wound healing processes like neovascularization. DCM biomaterial strength allows HSE graft transport and placement directly onto the wound from the *in vitro* cultures, avoiding problems with surgical handling. The random fiber orientation and DCM scaffold composition likely imparts stiffness that means wound contraction is less of an issue compared to other softer polymer materials where graft contraction can significantly limit the original surface area by as much as 20% [36].

Our data from experiment one, the excisional wounded animal model suggests that DCM scaffold alone is non-cytotoxic with dermal tissue and does not induce a foreign body immune response. This is in contrast to previous reports of electrospun fibers that only fail to induce acute foreign body immune responses when grafted with cells including: fibroblasts [34] and fibroblast/keratinocyte combinations in animal wounding models [22]. In the majority of these models the time frame for re-epithelialization to complete was within the critical two week period to reduce the chances of infection and subsequent hypertrophic scarring [22,24,34]. Wounded mouse models exhibit very different wounding time frame and responses from our previously described porcine model of burn wounding [37]. These differences relate to the scale of tissue, wounds and the differential structural composition of mouse skin resulting in healing largely by wound contraction, rather than re-epithelialization.

These factors are also likely to be important when assessing data from experiment two where DCM scaffold overcame the detrimental effects of grafting with the Nylon Mersilene™ mesh culture support with the DCM composite in inhibiting wound closure and promoting dermal thickening (it was included to support the DCM at the air liquid interface during culture to encourage keratinocyte differentiation). In future a better (less disruptive) alternative to mesh support will be identified for supporting scaffold composites, one that is hopefully easier to remove from the composites before grafting or a material that has less influence wound healing than the Nylon Mersilene™ mesh.

## 5. Conclusions

In conclusion, our data taken together show that DCM scaffold exhibits improved mechanical properties in terms of support and reducing graft shrinkage over unsupported cultured epithelial autografts (CEA) and avoids typical artificial polymer based scaffold immune responses. Furthermore, DCM cultured cell grafts do not require any donor site biopsies avoiding subsequent donor wounds as split thickness skin grafts procedures do. Further work would be beneficial to optimize keratinocyte adhesion, migration, proliferation and differentiation on DCM biomaterial to further improve its surface characteristics.

## Acknowledgments

This work was funded by a New Staff Start-Up Grant from The University of Queensland (JRM), by a grant-in-aid from the Health and Labor Sciences Research Grant (research into specific diseases) H17-Saisei-12 (Japan) and by support from the Brisbane Royal Children's Hospital Foundation (Queensland Children's Medical Research Institute, QCMRI). Author Disclosure Statement: The authors state that no completing financial interests exist.

## Appendix. Supplementary data

The supplementary data associated with this article can be found in the on-line version at doi:10.1016/j.biomaterials.2011.03.023.

## References

[1] Tanner Jr JC, Vandeput J, Olley JF. The mesh skin graft. Plast Reconstr Surg 1964;34:287–92.
[2] Warden GD, Saffle JR, Kravitz M. A two-stage technique for excision and grafting of burn wounds. J Trauma 1982;22:98–103.
[3] Boyce ST, Kagan RJ, Greenhalgh DG, Warner P, Yakuboff KP, Palmieri T, et al. Cultured skin substitutes reduce requirements for harvesting of skin autograft for closure of excised, full-thickness burns. J Trauma 2006;60:821–9.
[4] Yannas IV, Burke JF, Orgill DP, Skrabut EM. Wound tissue can utilize a polymeric template to synthesize a functional extension of skin. Science 1982;215:174–6.
[5] MacNeil S. Progress and opportunities for tissue-engineered skin. Nature 2007;445:874–80.
[6] Metcalfe AD, Ferguson MW. Tissue engineering of replacement skin: the crossroads of biomaterials, wound healing, embryonic development, stem cells and regeneration. J R Soc Interface 2007;4:413–37.
[7] Metcalfe AD, Ferguson MW. Bioengineering skin using mechanisms of regeneration and repair. Biomaterials 2007;28:5100–13.
[8] Berthod F, Germain L, Li H, Xu W, Damour O, Auger FA. Collagen fibril network and elastic system remodeling in a reconstructed skin transplanted on nude mice. Matrix Biol 2001;20:463–73.
[9] McMillan JR, Akiyama M, Tanaka M, Yamamoto S, Goto M, Abe R, et al. Small-diameter porous poly (epsilon-caprolactone) films enhance adhesion and growth of human cultured epidermal keratinocyte and dermal fibroblast cells. Tissue Eng 2007;13:789–98.
[10] Geisler HP. Biomaterials; 1996:17.
[11] Vacanti JP, Vacanti CA. In: Diego San, editor. Principles of tissue engineering. 2nd ed. CA, USA: Academic Press (Elsevier); 2000.
[12] Park SN, Park JC, Kim HO, Song MJ, Suh H. Characterization of porous collagen/hyaluronic acid scaffold modified by 1-ethyl-3-(3-dimethylaminopropyl)carbodiimide cross-linking. Biomaterials 2002;23:1205–12.
[13] Hafemann B, Ghofrani K, Gattner HG, Stieve H, Pallua N. Cross-linking by 1-ethyl-3- (3-dimethylaminopropyl)-carbodiimide (EDC) of a collagen/elastin membrane meant to be used as a dermal substitute: effects on physical, biochemical and biological features in vitro. J Mater Sci Mater Med 2001;12:437–46.
[14] Shields KJ, Beckman MJ, Bowlin GL, Wayne JS. Mechanical properties and cellular proliferation of electrospun collagen type II. Tissue Eng 2004;10:1510–7.
[15] Dai NT, Williamson MR, Khammo N, Adams EF, Coombes AG. Composite cell support membranes based on collagen and polycaprolactone for tissue engineering of skin. Biomaterials 2004;25:4263–71.
[16] Dai NT, Yeh MK, Liu DD, Adams EF, Chiang CH, Yen CY, et al. A co-cultured skin model based on cell support membranes. Biochem Biophys Res Commun 2005;329:905–8.
[17] Powell HM, Boyce ST. Engineered human skin fabricated using electrospun collagen-PCL blends: morphogenesis and mechanical properties. Tissue Eng Part A 2009;15:2177–87.
[18] Barnes CP, Pemble CW, Brand DD, Simpson DG, Bowlin GL. Cross-linking electrospun type II collagen tissue engineering scaffolds with carbodiimide in ethanol. Tissue Eng 2007;13:1593–605.
[19] Reneker DH, Yarin AL, Fong H, Koombhongse S. Bending instability of electrically charged liquid jets of polymer solutions in electrospinning. J Appl Phys 2000;87:4531–47.
[20] Reneker DH, Chun I. Nanometre diameter fibres of polymer, produced by electrospinning. Nanotechnology 1996;7:216–23.

[21] Matthews JA, Wnek GE, Simpson DG, Bowlin GL. Electrospinning of collagen nanofibers. Biomacromolecules 2002;3:232–8.
[22] Rho KS, Jeong L, Lee G, Seo BM, Park YJ, Hong SD, et al. Electrospinning of collagen nanofibers: effects on the behavior of normal human keratinocytes and early-stage wound healing. Biomaterials 2006;27:1452–61.
[23] Powell HM, Supp DM, Boyce ST. Influence of electrospun collagen on wound contraction of engineered skin substitutes. Biomaterials 2008;29:834–43.
[24] Powell HM, Boyce ST. Fiber density of electrospun gelatin scaffolds regulates morphogenesis of dermal-epidermal skin substitutes. J Biomed Mater Res A 2008;84:1078–86.
[25] Klingenberg JM, McFarland KL, Friedman AJ, Boyce ST, Aronow BJ, Supp DM. Engineered human skin substitutes undergo large-scale genomic reprogramming and normal skin-like maturation after transplantation to athymic mice. J Invest Dermatol 2010;130:587–601.
[26] Gawronska-Kozak B, Bogacki M, Rim JS, Monroe WT, Manuel JA. Scarless skin repair in immunodeficient mice. Wound Repair Regen 2006;14:265–76.
[27] Matthews JA, Boland ED, Wnek GE, Simpson DG, Bowlin GL. Electrospinning of collagen type II: a feasibility study. J Bioact Compat Polym 2003;18:125–34.
[28] Boukamp P, Petrussevska RT, Breitkreutz D, Hornung J, Markham A, Fusenig NE. Normal keratinization in a spontaneously immortalized aneuploid human keratinocyte cell line. J Cell Biol 1988;106:761–71.
[29] Swope VB, Supp AP, Greenhalgh DG, Warden GD, Boyce ST. Expression of insulin-like growth factor I by cultured skin substitutes does not replace the physiologic requirement for insulin in vitro. J Invest Dermatol 2001;116:650–7.
[30] Butler CE, Orgill DP, Yannas IV, Compton CC. Effect of keratinocyte seeding of collagen-glycosaminoglycan membranes on the regeneration of skin in a porcine model. Plast Reconstr Surg 1998;101:1572–9.
[31] Richardson KC, Jarret L, Finke EH. Embedding in epoxy resins for ultrathin sectioning in electron microscopy. Stain Technol 1960;35:313–23.
[32] Liu PY, Phillips GE, Kempf M, Cuttle L, Kimble RM, McMillan JR. Cyanoacrylate glue as an alternative mounting medium for resin-embedded semithin sections. J Electron Microsc (Tokyo) 2009;59:87–90.
[33] Zhao Y, Shimizu T, Nishihira J, Koyama Y, Kushibiki T, Honda A, et al. Tissue regeneration using macrophage migration inhibitory factor-impregnated gelatin microbeads in cutaneous wounds. Am J Pathol 2005;167:1519–29.
[34] Lee SB, Kim YH, Chong MS, Hong SH, Lee YM. Study of gelatin-containing artificial skin V: fabrication of gelatin scaffolds using a salt-leaching method. Biomaterials 2005;26:1961–8.
[35] Usha R, Ramasami T. The effects of urea and n-propanol on collagen denaturation: using DSC, circular dicroism and viscosity. Thermochimica Acta 2004;409:201–6.
[36] Fei X, Seah CS, Lee ST. Human keratinocyte cell culture for the burns patients—a preliminary report. Ann Acad Med Singapore 1991;20:493–7.
[37] Wang XQ, Liu PY, Kempf M, Cuttle L, Chang AH, Wong M, et al. Burn healing is dependent on burn site: a quantitative analysis from a porcine burn model. Burns 2009;35:264–9.

# Rapid immunochromatographic test for serum granulysin is useful for the prediction of Stevens-Johnson syndrome and toxic epidermal necrolysis

Yasuyuki Fujita, MD,[a] Naoya Yoshioka, MS,[a] Riichiro Abe, MD, PhD,[a] Junko Murata, MD, PhD,[a] Daichi Hoshina, MD,[a] Hirokatsu Mae, MS,[b] and Hiroshi Shimizu, MD, PhD[a]
*Sapporo, Japan*

***Background:*** Life-threatening adverse drug reactions such as Stevens-Johnson syndrome (SJS) and toxic epidermal necrolysis (TEN) sometimes start with clinical features of ordinary drug-induced skin reactions (ODSRs) and it may be difficult to make a correct diagnosis before severe mucocutaneous erosions occur. We have reported that serum granulysin levels are elevated (cut off: 10 ng/mL) in patients with SJS/TEN before generalized blisters form.

***Objective:*** We sought to develop a rapid detection system for elevated serum granulysin to predict the progression from ODSRs.

***Methods:*** Serum samples from 5 patients with SJS/TEN at 2 to 4 days before mucocutaneous erosions formed were analyzed. Sera from 24 patients with ODSRs and 31 healthy volunteers were also investigated as control subjects. We developed a rapid immunochromatographic assay for the detection of high levels of serum granulysin using two different antigranulysin monoclonal antibodies.

***Results:*** The immunochromatographic test showed positive results for 4 of 5 patients with SJS/TEN but only one patient of 24 with ODSRs. The results correlated closely with those of enzyme-linked immunosorbent assays.

***Limitations:*** The validation of the long-time stability in this test strip has not been investigated.

***Conclusion:*** This novel test enables the prediction of SJS/TEN occurrence in patients even when only features of ODSRs are noted clinically. (J Am Acad Dermatol 2011;65:65-8.)

***Key words:*** adverse drug eruption; diagnostic test; granulysin; Stevens-Johnson syndrome; toxic epidermal necrolysis.

Stevens-Johnson syndrome (SJS) and toxic epidermal necrolysis (TEN) are life-threatening adverse drug reactions characterized by blister formation and widespread skin detachment.[1] In the early stage, SJS/TEN presents clinically as edematous papules or erythema multiforme–like target rashes, which are very similar to those of ordinary drug-induced skin reactions (ODSRs). Such a clinical course makes it difficult to reach a diagnosis of SJS/TEN in the early stage, and this results in high mortality. There is an urgent need for a method to distinguish between early-stage SJS/TEN and ODSRs.

The method should be as fast as possible, because SJS/TEN usually occurs within a few days. Furthermore, the technique should be as clinically

*Abbreviations used:*

| | |
|---|---|
| ODSRs: | ordinary drug-induced skin reactions |
| sFasL: | soluble Fas ligand |
| SJS: | Stevens-Johnson syndrome |
| TEN: | toxic epidermal necrolysis |

From the Department of Dermatology, Hokkaido University Graduate School of Medicine,[a] and Sapporo Immuno Diagnostic Laboratory.[b]
The first two authors contributed equally to this article.
Funding sources: None.
Conflicts of interest: None declared.
Accepted for publication April 26, 2010.
Reprint requests: Riichiro Abe, MD, PhD, Department of Dermatology, Hokkaido University Graduate School of Medicine, N15 W7, Kita-ku, Sapporo 060-8638, Japan. E-mail: aberi@med.hokudai.ac.jp.
Published online April 20, 2011.
0190-9622/$36.00

doi:10.1016/j.jaad.2010.04.042

simple as possible, such as using immunochromatographic test strips that are available for the detection of influenza infections. Among several candidates for diagnostic markers, we examined soluble Fas ligand (sFasL) and found that it is elevated in the sera of patients with SJS/TEN in the early stage, before mucocutaneous erosions appear.[2,3] It would be very useful to be able to predict the occurrence of SJS/TEN, but sFasL serum levels are too low (cut off: 100 pg/mL) for use in a rapid diagnostic device.

Chung et al[4] recently reported that granulysin is highly expressed in blisters of patients with SJS/TEN. We found that both serum granulysin and sFasL are higher in patients with early-stage SJS/TEN than in patients with ODSRs.[5] Serum levels of granulysin are 100 times higher (cut off: 10 ng/mL) than those of sFasL. Based on these observations, we developed a rapid immunochromatographic assay for the detection of high-level serum granulysin to diagnose and predict the early stage of SJS/TEN.

**CAPSULE SUMMARY**

- Drug reactions sometimes start with edematous papules, and it may be difficult to distinguish life-threatening drug reactions from ordinary drug reactions early in their course.
- We recently found that serum granulysin levels are increased in patients who later develop Stevens-Johnson syndrome or toxic epidermal necrolysis.
- We report a novel immunochromatographic assay to detect high levels of serum granulysin. With this test, we can predict whether patients with nonspecific edematous papules will develop severe drug eruptions.

## METHODS

### Patients

SJS refers to cases with mucosal erosions and epidermal detachment of less than 10% of the body surface area, and TEN refers to those with more than 30% involvement. Disease onset in patients with SJS/TEN was defined as the day when the mucocutaneous or ocular lesion first eroded or ulcerated (day 1).[3] From multiple Japanese institutions, we obtained serum samples from 35 patients with SJS/TEN.[3] Of these, we investigated 5 patients whose sera had been collected before the diagnosis of SJS/TEN (day −2 to −4). The patient information is listed in Table I. Serum samples from patients with ODSRs (n = 24) and healthy volunteers (n = 31) were also analyzed. Informed consent was obtained from all patients, and the procedures were approved by the Ethical Committee of the Hokkaido University Graduate School of Medicine, Sapporo, Japan.

### Immunochromatographic assay

In the immunochromatographic test, a murine monoclonal antibody specific to human granulysin (RB1, MBL, Nagoya, Japan) was conjugated with microparticles and then placed on the glass membrane area of the test device in a dry state. Another granulysin monoclonal antibody (RC8, MBL) was immobilized on a nitrocellulose membrane to form a result line. Likewise, a control line was created by the immobilization of antimouse IgG. The granulysin in the serum sample specifically bound to the microparticles via RB1 and comigrated upward until the granulysin was sandwiched with the immobilized RC8, revealing a visible result line. The entire test procedure was completed within 15 minutes.

### Enzyme-linked immunosorbent assay

The granulysin concentrations of the serum samples were measured with a sandwich-enzyme-linked immunosorbent assay as previously described.[6,7] In brief, 96-well flat-bottomed plates were coated with 5 mg/mL of RB1 antibody and stored overnight at 4°C. The plates were then washed and blocked with phosphate-buffered saline containing 0.1% Tween-20 (washing buffer) and blocked with 10% fetal bovine serum in washing buffer at room temperature for 2 hours. The samples and standards (recombinant granulysin, R&D Systems, Minneapolis, MN) were incubated for 2 hours at room temperature. Then they were reacted with 0.1 mg/mL of biotinylated RC8 antibody for 1 hour. The plates were then treated with 0.2 mg/mL of horseradish-peroxidase-conjugated streptavidin (Roche Diagnostics, Basel, Switzerland) for 30 minutes at room temperature. The plates were incubated with tetramethylbenzidine substrate (Sigma, St Louis, MO) for 30 minutes at room temperature, and then 1 mol/L sulfuric acid was added. The optical density was measured at 450 nm using a microplate reader (Mithras LB940, Berthold Technologies, Thoiry, France).

## RESULTS

We first applied diluted recombinant human granulysin protein to the immunochromatographic test strips, to confirm the threshold and reliability of the assay. Approximately 10 ng/mL of sample yielded a result line, and 3 repeated investigations brought the same results (Fig 1, *A*).

**Table I.** Patient information

| Patient No. | Age, y | Sex | Diagnosis | Affected skin area | Causative drug | Serum granulysin (d) |
|---|---|---|---|---|---|---|
| 1 | 17 | M | SJS | 20% | Carbamazepine | 52.1 (−3) |
| 2 | 66 | F | TEN | 70% | Imatinib | 14.2 (−3) |
| 3 | 27 | F | SJS | <10% | Unknown | 42.2 (−4) |
| 4 | 80 | M | SJS | 5% | Phenytoin | 12.9 (−2) |
| 5 | 25 | F | SJS | Only mucosal lesions | Unknown | 2.7 (−2) |

*F*, Female; *M*, male; *SJS*, Stevens-Johnson syndrome; *TEN*, toxic epidermal necrolysis.

Based on this observation, we then applied serum samples to detect the elevated granulysin levels. Four of 5 SJS/TEN samples showed positive results (Fig 1, *B*). All the positive samples had elevated granulysin as detected by enzyme-linked immunosorbent assay analysis (30.35 ± 9.91 ng/mL, average ± SEM). The only sample with a negative result had granulysin at the normal level of 2.7 ng/mL. Conversely, one in 24 ODSRs samples and none of 31 healthy volunteers showed positive bands in this immunochromatographic assay. The test showed a sensitivity of 80% and a specificity of 95.8% for SJS/TEN versus ODSRs. The results of the immunochromatographic test correlated closely with early diagnosis for SJS/TEN ($P = 1.02 \times 10^{-3}$, analyzed by Fisher exact probability test).

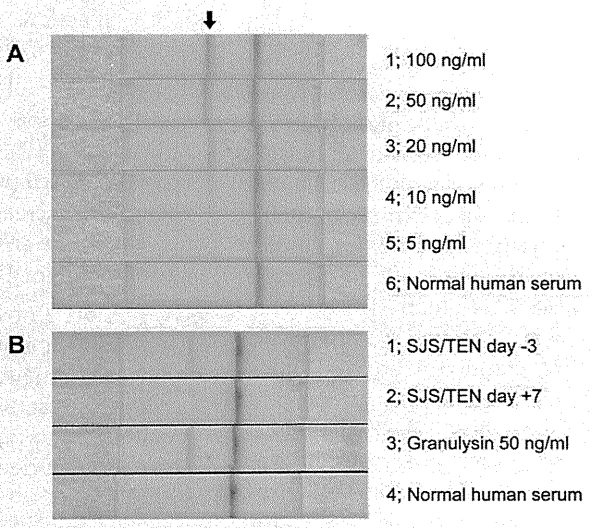


**Fig 1. A**, Immunochromatographic test strip detects elevated granulysin. *1 to 5*, Diluted recombinant granulysin is applied. *6*, Normal human serum as negative control (1.4 ng/mL). Positive results are shown as a band (indicated by the arrow). Approximately 10 ng/mL of granulysin is considered a positive result. **B**, Detection of serum granulysin by immunochromatographic assay. *1*, Serum taken from patient 1 with early Stevens-Johnson syndrome (*SJS*)/toxic epidermal necrolysis (*TEN*) 3 days before blister formation. Although patient showed only edematous erythema and papules without mucosal manifestations, serum granulysin was 52.1 ng/mL. *2*, Seven days after blister formation in same patient with SJS/TEN. No bands are observed, and serum granulysin has decreased to 5.7 ng/mL. *3*, Recombinant human granulysin as positive control. *4*, Normal human serum as negative control (3.5 ng/mL).

## DISCUSSION

We succeeded in developing a rapid immunochromatographic test for the detection of high-level serum granulysin that puts our previous findings to practical use. Although 20% of the cases could be missed, it would be a useful adjunct in diagnosing SJS/TEN. It would not be necessary for every morbilliform drug eruption. We suggest that the test be applied when clinical findings hinting at SJS/TEN, such as target lesions, are seen. However, two biopsies should be done as soon as SJS/TEN are suspected, for hematoxylin-eosin processing and immediate frozen sections, in order to look for necrotic keratinocytes, which is another sensitive test.[8] If the results of either method are negative, careful daily and hourly monitoring of the patient for a few days should take place. Furthermore, to assess the severity of illness and to predict mortality, we should use the mathematical tool called SCORTEN that has been developed.[9]

Granulysin, a member of the saposin-like protein family of lipid-binding proteins, exhibits potent cytotoxicity against a broad panel of microbial targets, including tumor cells, transplanted cells, bacteria, fungi, and parasites, damaging negatively charged cell membranes.[10] Granulysin plays important roles in host defense against pathogens, and it induces apoptosis of target cells in a mechanism involving caspases and other pathways.[11] Chung et al[4] reported that granulysin was identified as the most highly expressed cytotoxic molecule in blisters of patients with SJS/TEN. Very recently, we showed that granulysin levels of sera from patients with SJS/TEN are significantly elevated before the development of skin detachment or mucosal lesions.[5] The elevated serum granulysin levels decrease rapidly within 5 days after disease onset. This pattern is similar to that

observed with sFasL.[3] When granulysin levels for patients with SJS/TEN in the early stage were compared with those levels for patients with ODSRs and healthy control subjects, the differences were statistically significant.[5]

This novel test enables the early diagnosis of SJS/TEN in patients with cutaneous adverse drug reactions that are otherwise indistinguishable from ODSRs.

**REFERENCES**

1. Roujeau JC, Kelly JP, Naldi L, Rzany B, Stern RS, Anderson T, et al. Medication use and the risk of Stevens-Johnson syndrome or toxic epidermal necrolysis. N Engl J Med 1995;333:1600-7.
2. Abe R, Shimizu T, Shibaki A, Nakamura H, Watanabe H, Shimizu H. Toxic epidermal necrolysis and Stevens-Johnson syndrome are induced by soluble Fas ligand. Am J Pathol 2003;162:1515-20.
3. Murata J, Abe R, Shimizu H. Increased soluble Fas ligand levels in patients with Stevens-Johnson syndrome and toxic epidermal necrolysis preceding skin detachment. J Allergy Clin Immunol 2008;122:992-1000.
4. Chung WH, Hung SI, Yang JY, Su SC, Huang SP, Wei CY, et al. Granulysin is a key mediator for disseminated keratinocyte death in Stevens-Johnson syndrome and toxic epidermal necrolysis. Nat Med 2008;14:1343-50.
5. Abe R, Yoshioka N, Murata J, Fujita Y, Shimizu H. Granulysin as a marker for early diagnosis of the Stevens-Johnson syndrome. Ann Intern Med 2009;151:514-5.
6. Ogawa K, Takamori Y, Suzuki K, Nagasawa M, Takano S, Kasahara Y, et al. Granulysin in human serum as a marker of cell-mediated immunity. Eur J Immunol 2003;33:1925-33.
7. Saigusa S, Ichikura T, Tsujimoto H, Sugasawa H, Majima T, Kawarabayashi N, et al. Serum granulysin level as a novel prognostic marker in patients with gastric carcinoma. J Gastroenterol Hepatol 2007;22:1322-7.
8. Pereira FA, Mudgil AV, Rosmarin DM. Toxic epidermal necrolysis. J Am Acad Dermatol 2007;56:181-200.
9. Bastuji-Garin S, Fouchard N, Bertocchi M, Roujeau JC, Revuz J, Wolkenstein P. SCORTEN: a severity-of-illness score for toxic epidermal necrolysis. J Invest Dermatol 2000;115:149-53.
10. Kaspar AA, Okada S, Kumar J, Poulain FR, Drouvalakis KA, Kelekar A, et al. A distinct pathway of cell-mediated apoptosis initiated by granulysin. J Immunol 2001;167:350-6.
11. Clayberger C, Krensky AM. Granulysin. Curr Opin Immunol 2003;15:560-5.

Special Issue "Epithelial regeneration in inflammatory diseases"

Mini Review

# Regenerative medicine for severe congenital skin disorders: restoration of deficient skin component proteins by stem cell therapy

Yasuyuki Fujita*, Riichiro Abe, Wataru Nishie and Hiroshi Shimizu

Department of Dermatology, Hokkaido University Graduate School of Medicine, Sapporo, Japan

Some congenital skin disorders lacking structure proteins in the basement membrane zone carry severe prognosis because of severe erosion and skin dysfunction on the whole body. So far, several therapeutic strategies have been emerging for such disorders: 1. gene therapies, 2. protein therapies and 3. cell therapies. Cell therapies have a potential to affect skin systemically, and stem cell transplantation is one of the most hopeful candidates for treating severe congenital skin disorders such as epidermolysis bullosa, from a perspective of transdifferentiation and re-programming of stem cells. We review here the recent strategies and progress of stem cell transplantation for epidermolysis bullosa.

Rec./Acc.4/11/2011

*Correspondence should be addressed to:
Yasuyuki Fujita, Department of Dermatology, Hokkaido University Graduate School of Medicine, North 15 West 7, Kita-ku, Sapporo 060-8638, Japan. Tel: +81-11-706-7387 Fax: +81-11-706-7820 E-mail: yfujita@med.hokudai.ac.jp

**Key words:**
basement membrane zone, bone marrow transplantation, epidermolysis bullosa, stem cell therapy, type XVII collagen

## Introduction

The skin is the human body's largest organ and accounts for approximately 16% of an adult's body weight. Several critical roles owe to the skin, including moderation of body temperature, prevention from electrolyte loss and protection from physical stimuli. In order to resist mechanical stress, the skin has complicated structures connecting epidermis and dermis, called basement membrane zone (BMZ) or dermal-epidermal junction. The BMZ consists of more than 30 structure proteins to strengthen the adhesion (Fig. 1)[1], and one defect of these proteins by congenital abnormality or acquired autoimmunity cause skin fragility and blister formation immediately after mild mechanical stimuli. Blistering on the whole body extremely worsens the quality-of life and even causes death due to severe water loss and infections.

## Epidermolysis bullosa

One important example on the importance of BMZ proteins is epidermolysis bullosa (EB). EB comprises a group of inherited disorders in which the patient's epidermis can exhibit skin fragility caused by genetic abnormalities of a BMZ protein[2]. From the location of causative BMZ protein, EB is classified roughly into 3 categories: EB simplex (EBS), junctional EB (JEB) and dystrophic EB (DEB). Worldwide approximately 50 EB cases arise per a million live births and 92% accounts for EBS which is caused by cytokeratin 5/14 mutation with autosomal dominant inheritance[2]. Clinical manifestations vary broadly, from occasional mild erosion on the extremities to severe ulcers on the whole body or even stillbirth in Herlitz JEB and EBS/JEB with pyloric atresia. In recessive DEB, the most frequently recognized subtype in Japan, defect of type VII collagen (COL7) causes recurrent, deep erosions and ulcers on the extremities which results in mitten deformities and squamous cell carcinoma.

## Emerging novel strategies for EB treatment

Most prevalent treatments for EB patients are skin protective care, wound dressing agents and antibiotics against local infections. There have been no established and fundamental treatments because EB arises from gene mutations of keratinocytes and fibroblasts on the whole body. However, several novel strategies have been emerging for EB treatment recently: 1. gene therapies, 2. protein therapies and 3. cell therapies.

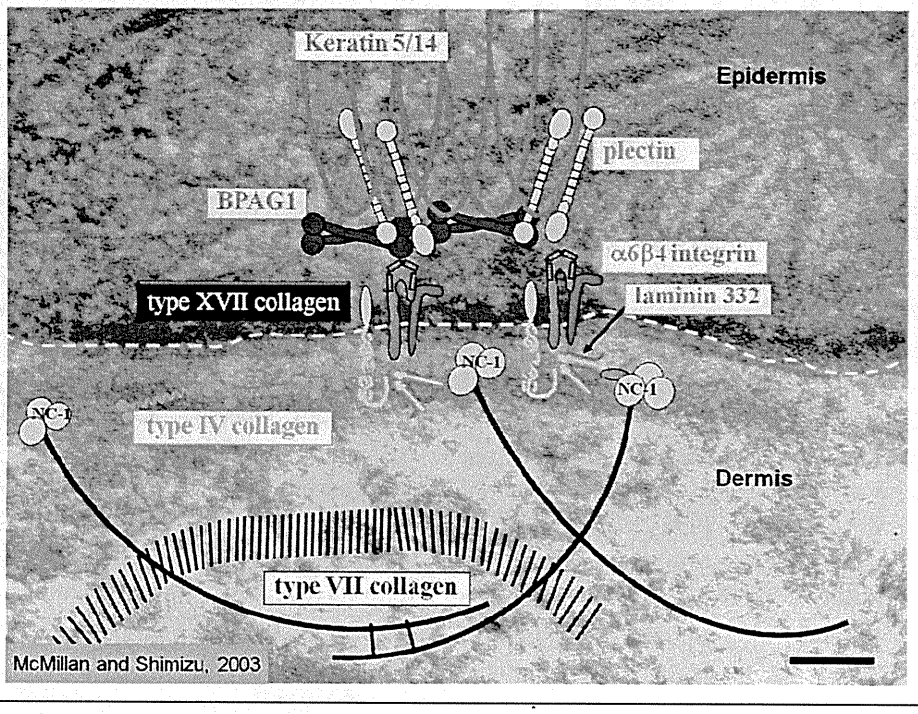


**Fig. 1**
Structure of basal membrane zone (BMZ) in the skin[1].

Gene therapies were performed by virus-mediated normal gene transfection into autologous keratinocytes, followed by cell culture to form epidermal sheet and grafting into the patients' skin. Such *ex vivo* gene-treated cultured autografting, reported by Mavilio *et al.*, is a promising therapeutic approach for junctional EB[3]. One of the merits of gene-mediated therapies is that autologous cells are fundamentally accepted without rejection response, except for the risk of immunoreactivity against the restored protein. Conversely, its effects are limited to the area of grafting and might be insufficient for systemic involvement of EB. Furthermore, the ethical and safety problems of using retroviruses for gene correction still exist[4]. Autologous induced pluripotent stem (iPS) cells are another source for gene therapies, since high proliferation potential provide enough number of differentiated cells without invasive techniques[5]. Successful treatment of sickle cell anemia model mice was recently reported by utilizing gene-corrected hematopoietic cell transplantation from autologous iPS cells[6]. Tolar *et al.* succeeded in the generation of autologous iPS cells from recessive DEB patient, which indicates that iPS-mediated therapies are theoretically possible by generation of epidermal/dermal sheets and hematopoietic stem cell transplantation[7]. However, ethical problems still lie on autologous iPS cells for the treatment of EB since gene correction by transfection is essential.

Conversely, few reports have been published as to *in vivo* gene therapies for EB[8]. As one candidate, several drugs have been reported to read through the specific stop codons of nonsense mutations, resulting in producing full-length proteins [9-11]. Therefore such "read-through" drugs might ameliorate severe congenital skin disorders if they are caused by the specific nonsense mutations. Since some subtypes of junctional EB have "hot spots" of nonsense mutations[12], there seems to be a space of novel gene-therapeutic agents in the future.

Congenital disorders that lack secretory proteins could be ameliorated by supplying the recombinant proteins systemically or locally. Several congenital metabolic disorders such as Fabry's disease have been already treated with enzyme replacement therapy[13]. Woodley and colleagues succeeded in the deposition of COL7 at the BMZ of artificially-constructed DEB skin by injecting recombinant COL7[14]. The same group later reported the amelioration of RDEB mice by injecting human COL7[15]. Other than secretory proteins like COL7, laminin beta-3, a structural protein in the BMZ, is found to be provided with protein therapy by protein transfection technique[16]. Protein therapies are safer than other novel therapies in the way that patients can attempt the therapy with lower dose of protein and that no gene correction is needed. Conversely, its effects are limited to the area of injection. The safety of the recombinant protein should be alarmed since bovine serum is generally essential for the culture of transfected cells. Efficient purification of large amount of protein is another challenge. The risk of immunoreactivity might weaken the effect of protein therapy and even cause exacerbation. In recessive DEB-generalized other type, the mutated COL7 protein partially function to form incomplete anchoring fibrils. Therefore, protein therapy-induced autoimmunity in such patients might inhibit the residual COL7 functions, resulting in exacerbation of blistering on the whole body.

Considering the clinical application of congenital disorders, the easiest source of normal proteins is allografts. Therefore, utilizing allogenic normal cells could be the fundamental therapeutic strategy. Applying allogenic keratinocytes, or allo-skin graft could treat congenital skin disorders, but allogenic keratinocytes are generally rejected because of their high immunogenicity. In order to overcome rejection, less immunogenic cells such as fibroblasts have been attempted to treat DEB. Intralesional injection of allogenic fibroblasts into DEB patients caused the deposition of COL7 for more than 3 months with matured anchoring fibrils[17]. Furthermore, intravenous injection of human fibroblasts into nude mice introduced human COL7 deposition in the BMZ of wound-healed skin[18]. Mesenchymal stem/stromal cells (MSCs) are another candidate for cell therapies; Conget and colleagues reported COL7 deposition at the site of intradermal injection of allogenic MSCs[19] in RDEB patient.

Another strategy of cell therapy is stem cell transplantation such as bone marrow transplantation (BMT) and cord-blood stem cell transplantation. If such stem cells engraft completely and provide functional stem cell-derived skin component cells from peripheral blood flow, systemic amelioration of EB will be accomplished for a long time without immunological rejection. Since stem cell transplantation has already performed widely for hematologic disorders and some congenital metabolic disorders, ethical and technical hurdles are much lower than gene/protein therapies.

## Differentiation from bone marrow cells into functional keratinocytes

Stem cells in the bone marrow were recently found to have a pluripotency; a potential to differentiate into various cell lineages other than hematocytes. This pluripotency or transdifferentiation are observed more frequently in the injured organs such as damaged liver, ischemic heart, injured nerve tissues and wounded skin[20,21]. However, it had been unknown what causes efficient differentiation from bone marrow stem cells into injured skin, and whether these differentiated cells actually function like other normal organ cells.

Our group first revealed that a chemokine CTACK/CCL27 from the injured skin tissue accelerates the differentiation from bone marrow stem cells into epidermal keratinocytes[22]. Murine GFP-positive bone marrow cells were transplanted into normal mice, and the acceleration of wound healing and GFP-positive epidermal keratinocytes were investigated with or without local injection of CTACK/CCL27. Interestingly, CTACK/CCL27 enhanced the bone marrow-derived keratinocytes approximately 4 times, which was inhibited by anti-CTACK/CCL27 antibodies. Another chemokine SLC/CCL21 are similarly found to enhance wound healing via differentiating MSCs into various skin component cells including keratinocytes[23].

We also revealed that these differentiated keratinocytes actually function and provide BMZ component proteins. Focused on one basal keratinocyte-specific structural protein type XVII collagen (COL17), we prepared mice expressing normal murine Col17 (mCol17), transgenic mice expressing both murine and human COL17 (hCOL17) and COL17-humanized mice that express only hCOL17[24]. Interestingly, the expressions of donor bone marrow-derived COL17 in the skin were confirmed after performing BMTs among these mice of different COL17 expression patterns[25]. Since only keratinocytes express COL17 among skin-component cells and peripheral blood, bone marrow-derived keratinocytes are found to function and produce a BMZ component COL17.

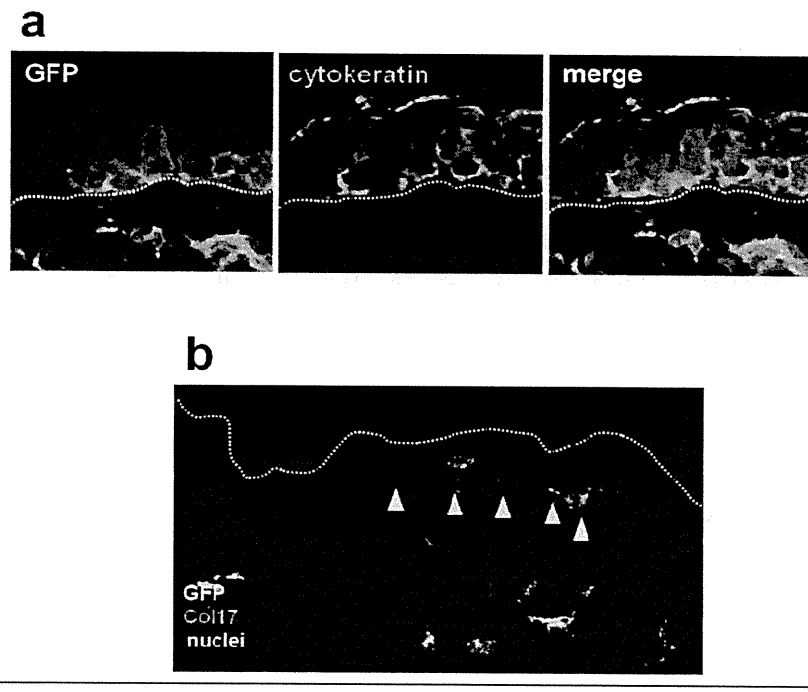


**Fig. 2**
Bone marrow transplantation into Col17 knockout JEB mice. (a) Donor-derived, GFP+ cytokeratin+ cells are aggregated in the basal cell layer of the epidermis, indicating bone marrow cells re-programmed into epidermal keratinocytes. (b) Immunofluorescence revealed GFP+ cells in the epidermis and dermis, with linear expression of Col17 in the BMZ.

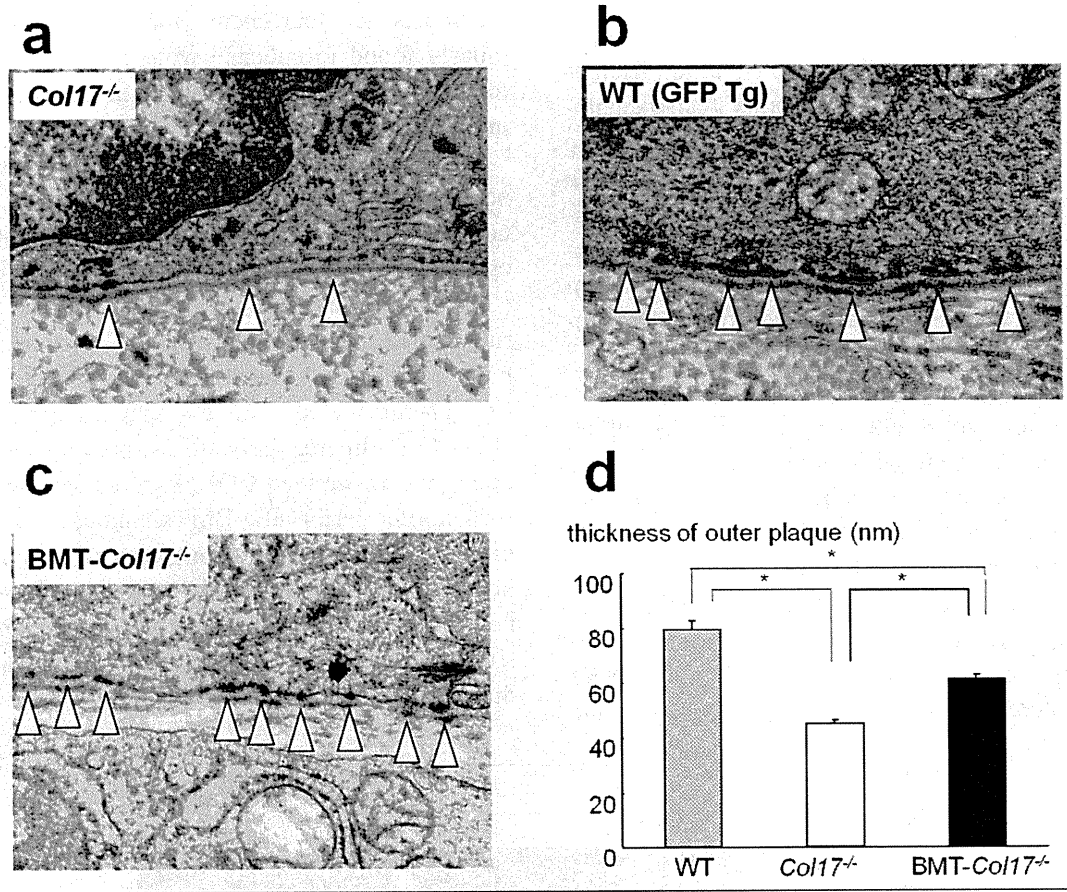


**Fig. 3**
Electron microscopy analysis in the skin after BMT into JEB mice. (a) Untreated Col17 knockout mice have thin, immature hemidesmosomes in the bottom of basal cell layer (arrowheads). (b) Normal C57BL/6 mice have mature, apparent hemidesmosomes. (c) Thick and matured hemidesmosomes are observed in the skin of BMT-treated Col17 knockout mice. (d) Thickness of the outer plaques of hemidesmosomes shows statistical improvement after BMT.

## Stem cell therapy for epidermolysis bullosa

As mentioned previously, stem cell therapy is a promising strategy for systemic amelioration of EB for a long time. So far, a few investigations of BMT to treat RDEB have been published. Tolar *et al.* reported that hematopoietic stem cells contributed to life prolongation in RDEB model mice[26]. Chino *et al.* reported that treatment of embryonic BMT into RDEB model mice induced the expression of type VII collagen[27]. These reports proved the existence of donor-derived fibroblasts by immunohistochemistry and cell culture, and these fibroblasts are thought to produce type VII collagen. Based on these findings, hematopoietic stem cell therapies recently performed for RDEB patients in the US as a phase I/II clinical trial[28]. Five out of seven patients survived after the treatment, and less frequent dressings into the wound skin have achieved probably due to restoration of type VII collagen. These reports implied the benefit of stem cell transplantation in patients with deficient type VII collagen, which is produced by both epidermal keratinocytes and dermal fibroblasts[29]. Then, how is the clinical effect of stem cell transplantation in other subtype of EB, in which keratinocyte-specific skin component protein is lacked?

In order to answer the question we performed stem cell transplantation into adult Col17 knockout JEB model mice[25]. These treated mice expressed the lacked Col17 protein in the BMZ of the eroded skin around donor-derived GFP+ keratinocytes, with mature hemidesmosomes on the basal cells (Fig. 2, 3).

Clinical manifestations such as skin fragility and survival rates were also improved after stem cell transplantation (Fig. 4). Not only conventional BMT technique but hematopoietic stem cells transplantation and MSC infusion improved the expression of Col17. Furthermore, human hematopoietic stem cells also have a potential to restore epidermal component proteins by investigation of human-murine xeno-transplantation model, which implies stem cell transplantation might be a promising and fundamental therapeutic strategy for the treatment of severe EB patients.

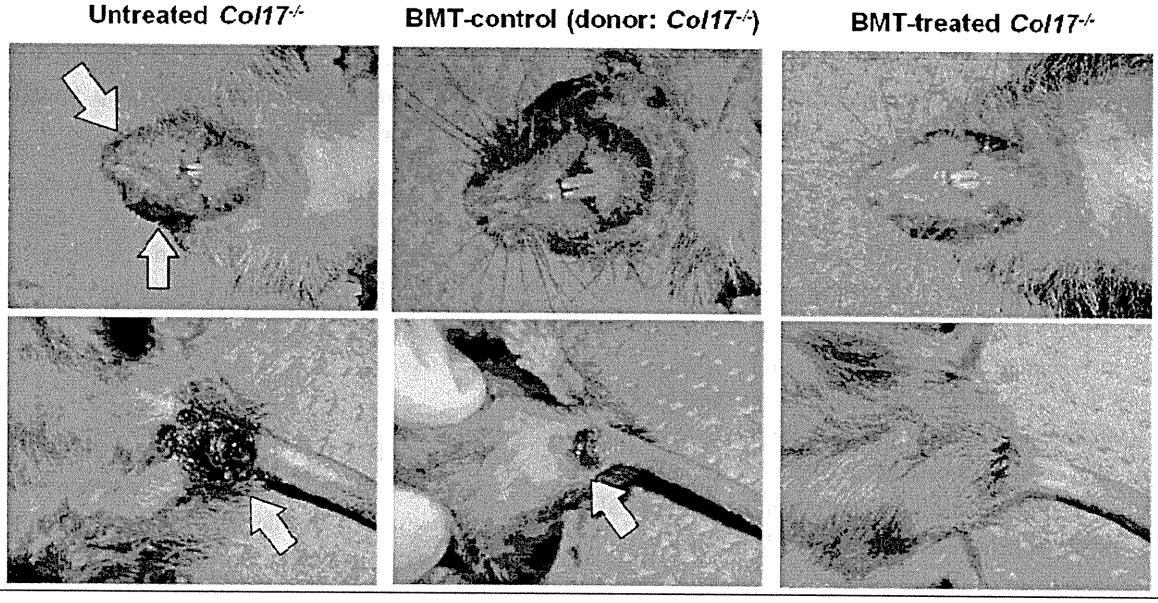


**Fig. 4**
Clinical manifestations of Col17 knockout mice after 120 days after birth (90 dayes after BMT). (left) Untreated Col17 knockout mice show erosions and ulcers on the perioral and perianal areas, which is compatible with clinical manifestations of JEB. (middle) As a control, BMT was performed from Col17 knockout mice into Col17 knockout mice. Severe erosions still appear as untreated mice. (right) Therapeutic BMT from GFP+ mice caused less severe erosions.

There still have problems to overcome on the stem cell transplantation for severe EB patients; *e.g.* risk of infection, conditioning regimens and donor supply. Although stem cell transplantation is prevalent, treatment-related deaths do occur due to severe infection, regimen-related toxicity and graft-versus-host disease (GVHD). Since EB patients have severe erosion and blisters on the whole body, severe cutaneous infections during the treatment could be fatal[28,30]. Conditioning regimens and the consideration of mini-transplantation should be determined carefully to avoid severe GVHD; both GVHD and regimen-related toxicity could cause severe erosions that are indistinguishable from EB symptoms. The donor is another challenge. Related HLA-matched siblings without EB phenotype are ideal for donors, but few cases meet the condition[28]. Unrelated HLA-matched stem cells from donor coordination programs, T-cell depleted haploidentical stem cell transplantation and iPS cell-bank projects might open the door to stem cell therapies in the future[31,32].

## Concluding remarks

Stem cell therapies have been emerged as a promising strategy for congenital severe skin disorders such as EB. Although merits and demerits should be considered compared to gene therapies and protein therapies, novel treatments from the view of regenerative medicine will be one of the main streams to provide fundamental answers for severe disorders.

## References

1) Shimizu H: Structure and Function of the Skin. Shimizu's Textbook of Dermatology, Nakayama Shoten Co., Ltd., Tokyo. 2007; 6.

2) Fine JD, Eady RA, Bauer EA, Bauer JW, Bruckner-Tuderman L, Heagerty A, Hintner H, Hovnanian A, Jonkman MF, Leigh I, McGrath JA, Mellerio JE, Murrell DF, Shimizu H, Uitto J, Vahlquist A,

Woodley D, Zambruno G: The classification of inherited epidermolysis bullosa (EB): Report of the Third International Consensus Meeting on Diagnosis and Classification of EB. J Am Acad Dermatol. 2008; 58: 931-950.

3) Mavilio F, Pellegrini G, Ferrari S, Di Nunzio F, Di Iorio E, Recchia A, Maruggi G, Ferrari G, Provasi E, Bonini C, Capurro S, Conti A, Magnoni C, Giannetti A, De Luca M: Correction of junctional epidermolysis bullosa by transplantation of genetically modified epidermal stem cells. Nat Med. 2006; 12: 1397-1402.

4) Gabriel R, Eckenberg R, Paruzynski A, Bartholomae CC, Nowrouzi A, Arens A, Howe SJ, Recchia A, Cattoglio C, Wang W, Faber K, Schwarzwaelder K, Kirsten R, Deichmann A, Ball CR, Balaggan KS, Yanez-Munoz RJ, Ali RR, Gaspar HB, Biasco L, Aiuti A, Cesana D, Montini E, Naldini L, Cohen-Haguenauer O, Mavilio F, Thrasher AJ, Glimm H, von Kalle C, Saurin W, Schmidt M: Comprehensive genomic access to vector integration in clinical gene therapy. Nat Med. 2009; 15: 1431-1436.

5) Takahashi K, Yamanaka S: Induction of pluripotent stem cells from mouse embryonic and adult fibroblast cultures by defined factors. Cell. 2006; 126: 663-676.

6) Hanna J, Wernig M, Markoulaki S, Sun CW, Meissner A, Cassady JP, Beard C, Brambrink T, Wu LC, Townes TM, Jaenisch R: Treatment of sickle cell anemia mouse model with iPS cells generated from autologous skin. Science. 2007; 318: 1920-1923.

7) Tolar J, Xia L, Riddle MJ, Lees CJ, Eide CR, McElmurry RT, Titeux M, Osborn MJ, Lund TC, Hovnanian A, Wagner JE, Blazar BR: Induced pluripotent stem cells from individuals with recessive dystrophic epidermolysis bullosa. J Invest Dermatol. 2011; 131: 848-856.

8) De Luca M, Pellegrini G, Mavilio F: Gene therapy of inherited skin adhesion disorders: a critical overview. Br J Dermatol. 2009; 161: 19-24.

9) Kerem E, Hirawat S, Armoni S, Yaakov Y, Shoseyov D, Cohen M, Nissim-Rafinia M, Blau H, Rivlin J, Aviram M, Elfring GL, Northcutt VJ, Miller LL, Kerem B, Wilschanski M: Effectiveness of PTC124 treatment of cystic fibrosis caused by nonsense mutations: a prospective phase II trial. Lancet. 2008; 372: 719-727.

10) Lai CH, Chun HH, Nahas SA, Mitui M, Gamo KM, Du L, Gatti RA: Correction of ATM gene function by aminoglycoside-induced read-through of premature termination codons. Proc Natl Acad Sci U S A. 2004; 101: 15676-15681.

11) Wilschanski M, Yahav Y, Yaacov Y, Blau H, Bentur L, Rivlin J, Aviram M, Bdolah-Abram T, Bebok Z, Shushi L, Kerem B, Kerem E: Gentamicin-induced correction of CFTR function in patients with cystic fibrosis and CFTR stop mutations. N Engl J Med. 2003; 349: 1433-1441.

12) Posteraro P, De Luca N, Meneguzzi G, El Hachem M, Angelo C, Gobello T, Tadini G, Zambruno G, Castiglia D: Laminin-5 mutational analysis in an Italian cohort of patients with junctional epidermolysis bullosa. J Invest Dermatol. 2004; 123: 639-648.

13) Desnick RJ, Brady R, Barranger J, Collins AJ, Germain DP, Goldman M, Grabowski G, Packman S, Wilcox WR: Fabry disease, an under-recognized multisystemic disorder: expert recommendations for diagnosis, management, and enzyme replacement therapy. Ann Intern Med. 2003; 138: 338-346.

14) Woodley DT, Keene DR, Atha T, Huang Y, Lipman K, Li W, Chen M: Injection of recombinant human type VII collagen restores collagen function in dystrophic epidermolysis bullosa. Nat Med. 2004; 10: 693-695.

15) Remington J, Wang X, Hou Y, Zhou H, Burnett J, Muirhead T, Uitto J, Keene DR, Woodley DT, Chen M: Injection of recombinant human type VII collagen corrects the disease phenotype in a murine model of dystrophic epidermolysis bullosa. Mol Ther. 2009; 17: 26-33.

16) Igoucheva O, Kelly A, Uitto J, Alexeev V: Protein therapeutics for junctional epidermolysis bullosa: incorporation of recombinant beta3 chain into laminin 332 in beta3-/- keratinocytes in vitro. J Invest Dermatol. 2008; 128: 1476-1486.

17) Wong T, Gammon L, Liu L, Mellerio JE, Dopping-Hepenstal PJ, Pacy J, Elia G, Jeffery R, Leigh IM, Navsaria H, McGrath JA: Potential of fibroblast cell therapy for recessive dystrophic epidermolysis bullosa. J Invest Dermatol. 2008; 128: 2179-2189.

18) Woodley DT, Remington J, Huang Y, Hou Y, Li W, Keene DR, Chen M: Intravenously injected human fibroblasts home to skin wounds, deliver type VII